Journal of Quantitative Spectroscopy & Radiative Transfer 318 (2024) 108948

Contents lists available at ScienceDirect

Journal of Quantitative Spectroscopy and Radiative Transfer

journal homepage: www.elsevier.com/locate/jqsrt

# The collision-induced absorption of $H_2$ near 1.20 μm: Subatmospheric measurements and validation tests of calculations

A.O. Koroleva [a,b], S. Kassi [a], H. Fleurbaey [a], A. Campargue [a,*]

[a] Univ. Grenoble Alpes, CNRS, LIPhy, Grenoble 38000, France
[b] A.V. Gaponov-Grekhov Institute of Applied Physics of the Russian Academy of Sciences, 46 Ulyanov Str., Nizhny Novgorod 603950, Russia

ARTICLE INFO

*Key words:*
Collision-induced absorption
Molecular hydrogen
CIA
$H_2$
Absorption continua

ABSTRACT

The weak binary collision-induced absorption (CIA) of molecular hydrogen is measured at room temperature in the first overtone region near 1.20 μm. Binary absorption coefficients are derived by cavity ring down spectroscopy (CRDS) at 28 selected spectral points sampling the (2–0) band between 7974 and 8650 $cm^{-1}$. While all previous studies used high density samples, the sensitivity of the CRDS method allowed deriving accurate CIA by using pressure ramps of pure $H_2$ limited to a maximum pressure of 1 atm. After subtraction of the Rayleigh contribution, a purely quadratic pressure dependence is obtained for the absorption coefficient at each measurement point and the CIA binary coefficients are derived with a 1.5 % accuracy. The comparison to theoretical values widely used for astronomical applications shows deviations values between 5 and 25 %.

## 1. Introduction

As a result of dipole moments induced by molecular interactions, molecular hydrogen shows broad collision induced absorption (CIA) bands which are a major source of infrared opacity in dense planetary atmospheres and "cool" stellar objects. The ($v$-0) CIA bands mostly coincide with the ($v$-0) overtone bands of the $H_2$ molecule ($v$ is the vibrational quantum number). After the pioneer measurements of the $H_2$ CIA bands by Welsh et al. [1] and Herzberg [2], a general theory has rapidly emerged to account for the observations [3–6]. Molecular hydrogen being the simplest molecular systems, high level calculations from first principles have been continuously improved leading to sets of CIA cross-sections which are extensively used for the analysis of a variety of stellar objects [7–14]. Considering the broad ranges of temperatures of these objects (up to thousands of Kelvin) and the large frequency range from the rotational region to overtones bands in the visible, calculations are the only way to fulfil the needs. In a number of studies, these computed CIAs have been compared to available laboratory measurements for validation tests and a good agreement was generally observed from a visual superposition of the experimental and calculated CIA (frequently in logarithmic scale). We nevertheless note that in the most recent measurements of the (2–0) CIA, more than twenty years ago, Brodbeck et al. obtained significant (up to 30 %) discrepancies between experiment and theory but left open the origin of the differences [15]. This situation results from the fact that neither experimental nor computed CIA values are provided with error bars. To the best of our knowledge, the calculated CIA datasets largely used by astrophysicists have not yet been quantitatively validated by accurate measurements and their level of accuracy remains to be determined. The main purpose of the present work is to obtain accurate laboratory data for validation tests of the $H_2$ CIA in the first overtone region near 1.20 μm.

On the experimental side, CIA measurements in $H_2$ are not easy due to the weakness of the broad band absorption signal to be measured. In all previous measurements of the (2–0) CIA (see review in Table 1), the lack of sensitivity of traditional absorption techniques (Fourier transform spectroscopy or grating spectrograph) has been compensated by the use of high pressure gas cell (densities from 16 to 1500 amagat). In the above mentioned FTS study, Brodbeck et al. performed FTS recordings of the $H_2$ absorption spectrum for densities between 125 and 291 amagat (at 298 K) [15]. Significant deviations from the expected quadratic dependence of the CIA with density were evidenced. In this situation, Brodbeck et al. recommended as CIA binary cross-section values, the value of the absorption coefficient normalized by the squared gas density that they extrapolated at zero density. This study is, to the best of our knowledge, the only one in the (2–0) band where the pressure dependence of the absorption coefficient was carefully investigated. All the other previous (2–0) CIA determinations were based on

* Corresponding author.
*E-mail address:* alain.campargue@univ-grenoble-alpes.fr (A. Campargue).

https://doi.org/10.1016/j.jqsrt.2024.108948
Received 12 January 2024; Received in revised form 16 February 2024; Accepted 16 February 2024
Available online 17 February 2024

**Table 1**
Review of the measurements of the (2–0) CIA of $H_2$ and corresponding experimental conditions and methods.

| Reference | Technique | Density (amagat) | $L$ (m) | $T$ (K) |
|---|---|---|---|---|
| Welsh1951 [1] | Grating | 150/1500 | 0.85/0.30 | 80, 300 |
| Watanabe1971 [16] | Grating | ?/?/31 | 13.6/0.6/0.25 | 24/195/300 |
| McKellar1971 [17] | Grating | 19.9–37.4 | 137 | 84–89 |
| Silvaggio1981 [18] | FTS | 20 | 12.43 and 36.75 | 122 and 273.3 |
| McKellar1988 [19] | Grating | 16–19 | 110 | 28 |
| Brodbeck2001 [15] | FTS | 70–350 | 2.15 | 77.5, 298 |
| This work [a] | CRDS | 0–1 | | 294 |

Note.
[a] In [20], a first CRDS measurement was performed at subatmospheric pressure, at a single spectral point in the vicinity of the (2–0) Q(1) line near 8075 $cm^{-1}$ (see Text).

measurements at a single (high) density which hampers to discuss possible experimental biases and provide reliable error bars.

In the case of the (3–0) band, the absorption coefficient normalized by the squared gas density was also found to vary with the density, more precisely, to increase with densities in the 230–750 amagat range [21]. This increase was interpreted as due to the contribution of ternary collisions but a similar study of the (3–0) CIA reported by Brodbeck et al. for densities in the 200–1000 amagat range, showed that depending on the wavenumber, the deviations could be an increase or a decrease [22]. Let us note that the accuracy of the obtained zero density CIA is certainly affected by the very long range extrapolation from measurements at high densities, all above 125 amagat and 200 amagat for the (2–0) and (3–0) bands, respectively.

Nowadays, modern laser-based cavity enhanced techniques provide sufficient sensitivity for low density (<1 amagat) CIA measurements in the near infrared band of $H_2$. Because they are unaffected by three-body collision effects, the derived binary coefficients are expected to be more accurate and thus relevant for a direct comparison with theoretical values. In a recent work devoted to the binary absorption coefficients for $H_2$+$CO_2$ mixtures by cavity ring down spectroscopy (CRDS) in the 2.12–2.35 μm spectral region, $H_2$ CIA was determined from low pressure recordings (<400 Torr) at three spectral points of the (1–0) fundamental band (4250, 4430 and 4525 $cm^{-1}$) [23]. The experimental CIA values determined with an uncertainty of about 1 % were found lower by a few % compared to the calculated values from [7], recommended by the HITRAN database [24].

In the present work, we use the highly sensitive CRDS technique to determine CIA cross-sections at about 28 spectral points sampling a large part of the (2–0) CIA (7974–8650 $cm^{-1}$). Compared to the pressure conditions used with traditional methods (Table 1), the CIA amplitude at subatmospheric pressure is reduced by several orders of magnitude. As the CRDS technique is based on the monitoring of the variation of the losses of a high finesse optical cavity when the cavity is filled by hydrogen, it is necessary to ensure that the weak signal to be measured (maximum absorption coefficient of $7 \times 10^{-8}$ $cm^{-1}$ for a 1 amagat density) is not biased by small changes in the optical alignment of the CRDS setup induced by the pressure variation. In the following Part 2, we will present the experimental procedure used to measure the pressure dependence of the $H_2$ CIA at fixed spectral points, during pressure ramps up to 1 atm. Part 3 will be devoted to the retrieval of the binary CIA coefficients and to the comparison to previous works. Concluding remarks and perspectives will close the report (Part 4).

## 2. CRDS recordings and data analysis

Continuous-wave CRDS is a high-sensitivity technique for absorption spectroscopy based on a high-finesse cavity, the CRDS cell [25–27], giving a direct measurement of the extinction coefficient, $\alpha(\nu)$ (in $cm^{-1}$), at a wavenumber, $\nu$. The used CRDS spectrometer has been described in [28]. The CRDS cavity consists in two mirrors with highly reflective coatings separated by 142 cm. Two external cavity diode lasers (ECDL, Toptica fiber-connected DL pro) giving access to the 7960–8100 and 8100–8650 $cm^{-1}$ ranges were used as light sources. Laser light is injected in the cavity with the help of a single mode polarization-maintaining fiber. The output mirror of the cavity is mounted on a piezoelectric transducer (PZT) allowing for dithering the cavity length and thus obtaining resonance between the light and one of the longitudinal modes of the optical cavity. At resonance, the laser light entering the cavity is switched off with an acousto-optic modulator (FCM series from Intra Action, 40 MHz, 0.5 W RF). The purely exponential decay of light intensity is measured by an InGaAs PIN photodiode and the ring down (RD) time, $\tau$, corresponding to the decay time of photons leaking from the cavity is obtained from a fit. A CRDS spectrum is obtained as the variation of the loss rate, $\frac{1}{c\tau_0}$, as a function of the laser frequency. In the present recordings, for the evacuated cavity, the RD time, $\frac{1}{c\tau_0}$, varied from about 180 to 360 μs depending on the wavenumber. This leads to a minimum detectable absorption coefficient of about $1 \times 10^{-11}$ $cm^{-1}$.

Assuming that the optical alignment is unaffected by the gas injection, the additional loss rate induced by the gas filling the cavity, $\alpha(\nu)$ (in $cm^{-1}$), is obtained by difference of the loss rates obtained with the filled cell and with the evacuated cell:

$$\alpha(\nu) = \frac{1}{c\tau} - \frac{1}{c\tau_0} \quad (1)$$

where $c$ is the speed of light (neglecting the refractive index of the gas, very close to 1). For simplicity, in the following, we will call $\alpha(\nu)$ "absorption coefficient" while it involves a contribution due to Rayleigh scattering. In the present experiment, $\alpha(\nu)$ is the sum of three contributions: the CIA, the losses due to Rayleigh scattering and possibly, the absorption of rovibrational lines:

$$\alpha(\nu) = \alpha_{CIA}(\nu) + \alpha_{Rayleigh}(\nu) + \alpha_{Line}(\nu) \quad (2)$$

The CIA term can be expressed as $\alpha_{CIA}(\nu) = B(\nu)\rho_{H_2}^2$ where $\rho_{H_2}$ is the molecular density in amagat and $B_{CIA}$ is the binary collision absorption coefficient in $cm^{-1}amagat^{-2}$. Losses due to Rayleigh diffusion are small but not negligible compared to the CIA. They can be evaluated using an approximate empirical cross section of $8.49 \times 10^{-45}$ $\nu^{-4}$ $cm^2$ [29]. As concerns rovibrational lines, $H_2$ spectrum is very sparse and consists of very weak electric quadrupole transitions with well-known position [30]. In the present work, the spectral points of the measurements were chosen distant from the $H_2$ lines making negligible the contribution of $H_2$ line profiles. Let us mention that previous CIA determinations were obtained in our group as "side-product" of accurate CRDS measurement of two $H_2$ lines: (1–0) S(2) at 4917 $cm^{-1}$ [31] and (2–0) Q(1) at 8075 $cm^{-1}$ [20]. In these works, fits of the $H_2$ line profiles recorded at several pressures using sophisticated line shapes yielded not only the line parameters but also the baseline level due to the CIA allowing the determination of the CIA cross sections.

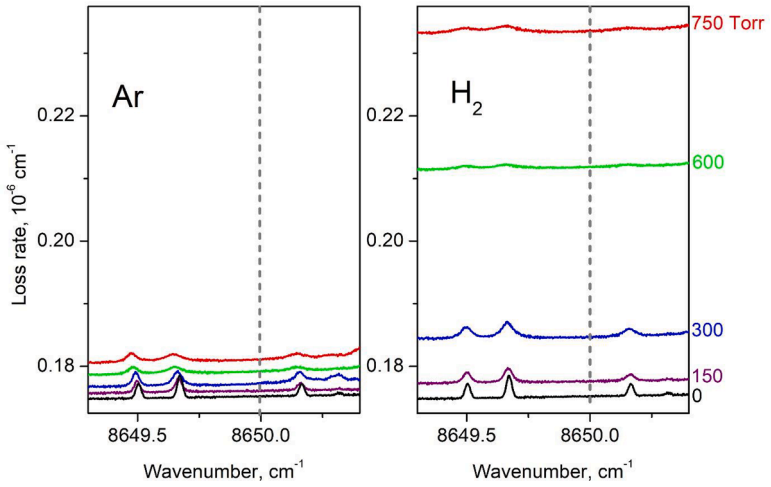


**Fig. 1.** Pressure dependence of the CRDS spectra of Ar (left panel) and $H_2$ (right panel) near 8650 $cm^{-1}$ for different pressure values up to 750 Torr. The dashed line marks one of the measurement points of the CIA using pressure ramps. The observed lines broadened by pressure are due to water vapor present as an impurity in the CRDS cell.

Possible contribution of lines due to water desorbing from the CRDS setup has to be considered as they are observed in the spectra (Fig. 1). Indeed, the considered spectral region corresponds to strong absorption bands of water vapor, with line intensities more than five orders of magnitude stronger than that of the (2–0) $H_2$ lines. Spectra simulations using the HITRAN database and CRDS recordings were used to ensure that the chosen spectral points are free from water vapor absorption. In Fig. 1, the location of one of the measurement spectral points is indicated on a series of spectra recorded for five pressures of $H_2$ (Alphagaz2, 99.9999 % chemical purity) between 0 and 750 Torr. For comparison, the figure includes spectra recorded in the same conditions with Ar. The rapid increase of the baseline level of the $H_2$ spectra with pressure is (mostly) due to the CIA.

In order to sample the 7960 - 8650 $cm^{-1}$ interval accessible with the two available laser sources, 28 spectral points were selected at wavenumbers free of line absorption of $H_2$ or water vapor. For each spectral point, the CRDS loss rate was monitored during increasing and decreasing pressure ramps up to 1 atm. As the CIA shows up as an increase of the loss rate when the gas is injected into the high finesse cavity, it is necessary to check that the measurements are not biased by a change of the optical alignment induced by the pressure variation. In order to evaluate (and correct) this potential bias, measurements were performed for pressure ramps using argon instead of $H_2$ (Fig. 1). The system was pumped to a pressure of $10^{-2}$ Torr each time the gas was changed. Argon pressure ramps recorded before and after each $H_2$ ramp show good reproducibility indicating the absence of residual deformations affecting subsequent measurements. Being a non-absorbing gas, the variation of the loss rate during Ar ramps is only due to Rayleigh scattering and to the small optical deformation of the CRDS cell due to the pressure change. The Rayleigh scattering contribution in Ar can be easily calculated [32] and subtracted from the measured Ar loss rates in order to obtain the mechanical contribution. Assuming identical deformation of the cavity alignment for Ar and $H_2$, the Ar pressure ramps were used to correct the deformation effects during the $H_2$

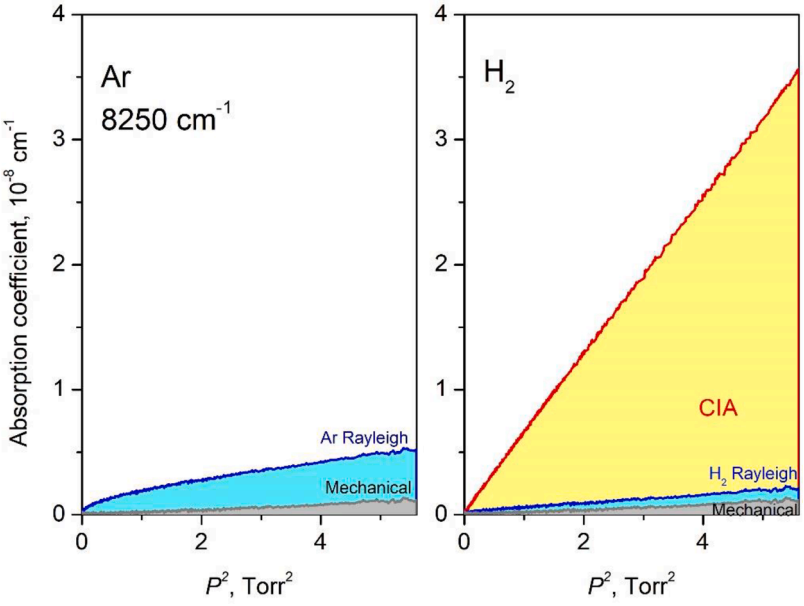


**Fig. 2.** Pressure dependence of the absorption measured by CRDS at 8250 $cm^{-1}$ during pressure ramps of argon and $H_2$ *versus* the squared pressure. The different contributions are separated: Rayleigh scattering (cyan), mechanical deformation deduced from the Ar ramp is assumed unchanged during $H_2$ ramp (grey) and CIA of $H_2$ (yellow). Note that the plotted measured absorption coefficient includes the deformation term which is omitted in Eqs. (1) and (2).

pressure ramps. The procedure is illustrated in Fig. 2 for the 8250 $cm^{-1}$ spectral point. The CIA is thus obtained from the $H_2$ loss rate after subtraction of the corresponding Rayleigh contribution and of the deformation contribution. Let us note that in Fig. 2 the different contributions are plotted *versus* the squared pressure, leading to a nonlinear variation for the Rayleigh contribution (which is proportional to the pressure) while the mechanical contribution appears to be mostly quadratic with pressure. This observation indicates that elastic mechanical deformation may induce losses with a nearly density squared variation, indistinguishable from the real CIA signal. According to Fig. 2, neglecting the mechanical effects would have led to an overestimation of the CIA by about 1.4 %.

In Fig. 3, the different contributions are plotted in logarithmic scale for all the measurement points. The deformation contribution is strongly dependent on the initial alignment of the setup but remains small. It represents 2.8 % of the measured signal in the worst cases (near 8300 $cm^{-1}$) but is negligible (about 0.2 %) in the 8400–8600 $cm^{-1}$ interval.

## 3. CIA cross-sections and comparison with literature

After subtraction of the Rayleigh and deformation contributions, for each spectral point, the pressure dependence of the CIA is obtained as illustrated in Fig. 4. On this graph, the signals obtained during the increasing and decreasing pressure ramps are superimposed (grey and colored lines, respectively). For all increasing and decreasing ramps, the agreement is within 2 %. We also checked that the results were unaffected by the gas flow during the ramps. The typical pressure variation was about 1 Torr/s corresponding to typical pressure ramp duration of about 12 min. Tests performed with pressure variation in the 0.3 – 3 Torr/s range showed that the results were insensitive to the gas flow.

The CIA term appearing in Eq. (2) can be expressed as $\alpha_{CIA}(\nu) = B_{CIA}(\nu)\rho_{H_2}^2$ where $\rho_{H_2}$ is the molecular density in amagat and $B_{CIA}(\nu)$ is the binary absorption coefficient in $cm^{-1}amagat^{-2}$. The binary coefficient at each spectral point was obtained from a linear fit of the corresponding CIA dependence *versus* the pressure squared. The retrieved

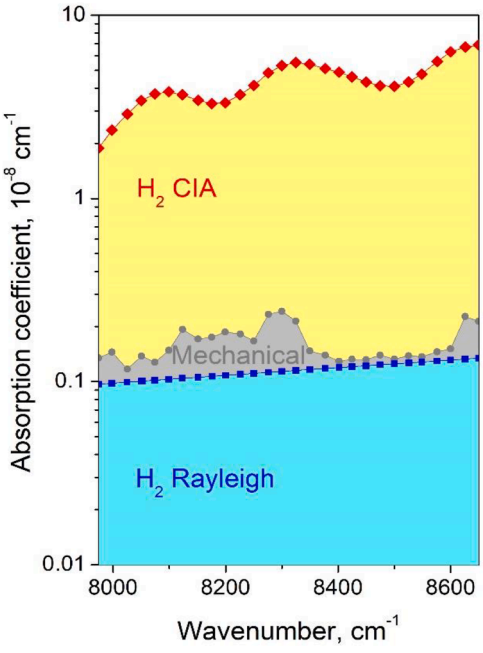


**Fig. 3.** Different contributions to the absorption coefficient of $H_2$ at 750 Torr measured by CRDS between 7960 and 8650 $cm^{-1}$: Rayleigh scattering (cyan), mechanical deformation (grey) and CIA (yellow). Note that the plotted measured absorption coefficient includes the deformation term which is omitted in Eqs. (1) and (2).

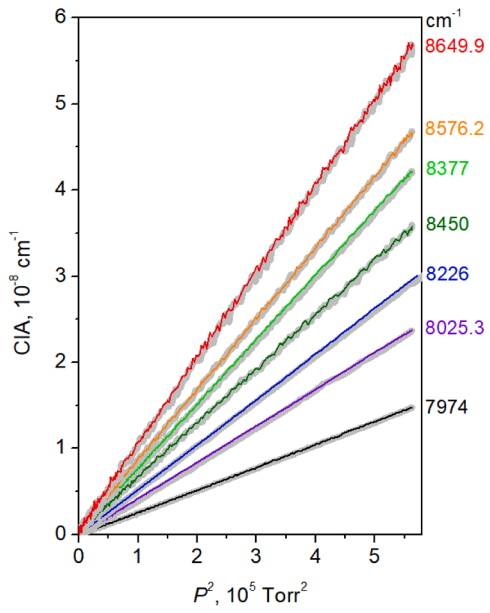


**Fig. 4.** CIA absorption coefficient *versus* the squared pressure of $H_2$ during pressure ramps for different spectral points near 1.2 μm. For each spectral point, measurements were performed during increasing and decreasing pressure ramps up to 750 Torr (grey and colored lines, respectively). The CIA cross-section binary coefficients were derived from the linear fits.

**Table 2**
CIA binary absorption coefficients at 293.5 K in the first overtone band of $H_2$.

| Wavenumber, $cm^{-1}$ | $B_{CIA}$, $10^{-8}$ $cm^{-1}amagat^{-2}$ |
|---|---|
| 7974.00 | 1.747(25) |
| 7998.00 | 2.214(9) |
| 8025.30 | 2.770(28) |
| 8050.30 | 3.281(28) |
| 8074.25 | 3.597(42) |
| 8099.05 | 3.676(27) |
| 8123.25 | 3.484(44) |
| 8151.00 | 3.266(40) |
| 8175.50 | 3.123(44) |
| 8199.50 | 3.148(17) |
| 8226.00 | 3.500(27) |
| 8250.20 | 3.966(14) |
| 8276.10 | 4.619(17) |
| 8300.20 | 5.068(17) |
| 8324.90 | 5.309(68) |
| 8349.50 | 5.255(41) |
| 8377.00 | 4.976(19) |
| 8401.80 | 4.757(33) |
| 8424.70 | 4.480(16) |
| 8450.00 | 4.185(14) |
| 8474.70 | 3.985(17) |
| 8500.00 | 3.959(15) |
| 8525.50 | 4.182(13) |
| 8548.70 | 4.643(17) |
| 8576.20 | 5.454(16) |
| 8600.15 | 6.169(29) |
| 8626.00 | 6.484(22) |
| 8649.90 | 6.663(17) |

$B_{CIA}$ values are listed in Table 2 and the obtained CIA frequency dependence is presented in Fig. 5. Note that during the whole measurement campaign, the temperature evolved between 19.5 and 21.8 °C, the average temperature value being 20.4 °C (293.5 K). According to the temperature dependence of the CIA provided by the HITRAN database [24], a 1 K temperature change leads to a maximum variation of the CIA of 0.2 %, although this value strongly depends on the wavenumber. The uncertainties included in the Table 2 correspond to a 1$\sigma$ standard

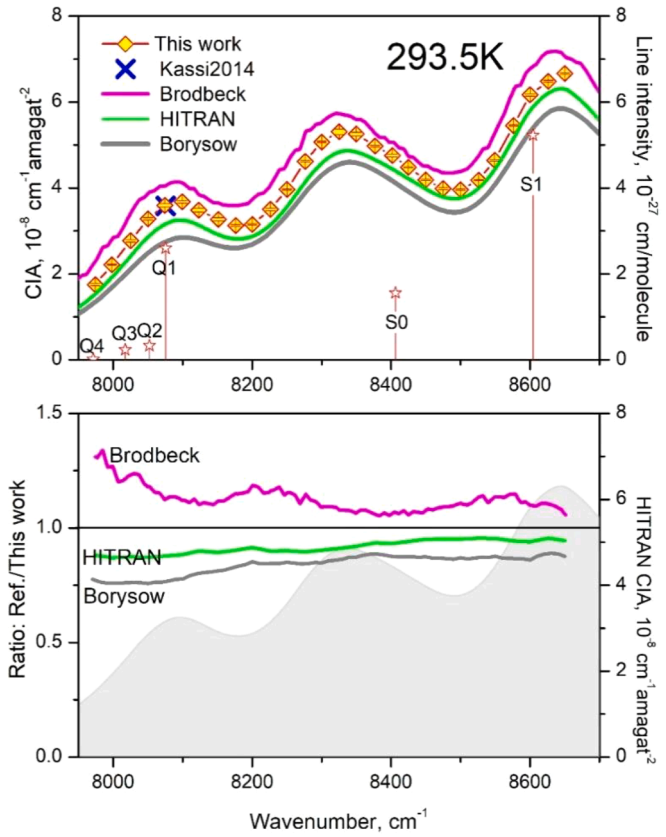


**Fig. 5.** Frequency dependence of the CIA binary coefficient at 293.5 K in the region of the (2–0) band of $H_2$ and comparison to previous works. The present CRDS measurements (yellow squares) are compared to calculated values recommended by the HITRAN database (grey line) or computed by Borysow (green line) [12]. Experimental values by Brodbeck et al. (pink line) were digitized from Fig. 3 of [15]. The CRDS value near 8075 cm$^{-1}$ (blue cross) was obtained in [20].

deviation. They accounted for (a) the experimental noise, deviations from quadratic pressure dependence and (b) the influence of the temperature deviation from the mean value of 293.5 K calculated with the temperature dependence given in the HITRAN database. For most of the chosen wavenumbers, the latter does not exceed 18 % of the total uncertainty (except the points at 7998, 8276.1, and 8525 cm$^{-1}$ where it reaches 23, 55 and 26 %, correspondingly).

We have included in Fig. 5, CIA binary coefficient recommended by the HITRAN database [24] and computed by Borysow [12]. HITRAN CIA datasets of $H_2$ reproduce the results of the calculations performed by Abel et al. [7] based on an improved interaction-induced dipole surface and a potential energy surface of collisionally interacting $H_2$ molecules. CIA datasets are provided at different temperatures between 200 and 3000 K, with a 25 K temperature step. The comparison of the CIA values at 275 and 300 K indicates that, except an increase up to 0.5 %/K below 8000 cm$^{-1}$, the temperature dependence is weak, less than 0.25 %/K in the entire range of our measurements. For a proper comparison to our results at 293.5 K, we have used HITRAN temperature dependence to extrapolate at 293.5 K all the literature sources displayed in Fig. 5, in particular the results of the calculations performed by Borysow [12] which have largely been adopted for astronomical applications.

The CIA ratios displayed in the lower panel of Fig. 5, indicates than on average both HITRAN and Borysow's modeling lead to CIA values systematically smaller than measured. In the 7960–8650 cm$^{-1}$ range of our study, the deviations vary between −13 % and −5 % for HITRAN values and between −25 % and −12 % for Borysow's results.

As concerns previous experimental results reviewed in Table 1, the only numerical $B_{CIA}$ value we found in the literature is that derived from the baseline variation of the CRDS spectra near the Q(1) (2–0) line at 8075.2 cm$^{-1}$ [20]. In that work, a series of spectra were recorded for five pressure values up to 640 Torr. The derived $B_{CIA}$ value of $3.58\times10^{-8}$ cm$^{-1}$amagat$^{-2}$ is in excellent agreement with the present value of $3.597\times10^{-8}$ cm$^{-1}$amagat$^{-2}$ obtained using pressure ramps at fixed frequency (namely 8074.25 cm$^{-1}$). In absence of extensive sets of experimental values obtained from high pressure measurements, we digitized the $B_{CIA}$ values displayed in Fig. 3 of [15] and included them in Fig. 5. Overall, these FTS measurements led to CIA values systematically larger than our values with deviations decreasing from 30 % near 7960 cm$^{-1}$ to about 5 % near 8500 cm$^{-1}$. Let us recall that, as detailed in the introduction, the CIA reported by Brodbeck et al. was obtained by extrapolation at zero density of measurements performed with densities between 125 and 291 amagat. Considering the very long range extrapolation, the achieved level of agreement can be considered as very satisfactory.

We have included in Fig. 5, the stick spectrum of the quadrupole transitions of the (2–0) band but the $H_2$ CIA is a superposition of the bands involving single (2–0) excitation of one $H_2$ molecule and double (1–0) excitation of two molecules (see for instance [16–18]). At room temperature, the resulting absorption structure extends from 7500 to 9200 cm$^{-1}$ [15]. At low temperature, the contributions of the single and double excitations can be partly resolved [15,16,18]. In our region, the (2–0) CIA shows three maxima around 8100, 8300 and 8650 cm$^{-1}$. The first one is mostly due to a single excitation corresponding to Q1 (2–0) while the two others involve a contribution of both single and double excitations: *(i)* S0 (2–0) and twice Q1 (1–0) near 8300 cm$^{-1}$ and *(ii)* S1 (2–0) and twice S0 (1–0) near 8650 cm$^{-1}$. We note that the deviations between calculations and measurements are very smooth *versus* frequency and thus mostly independent of the excitation involved.

To the best of our knowledge, no extensive study has been yet dedicated for low pressure CIA measurements in the (1–0) fundamental band. As mentioned above, in [23], $B_{CIA}$ values were determined by CRDS at three spectral points of the (1–0) band (4250, 4430 and 4525 cm$^{-1}$) with an uncertainty of about 1 % and found lower than HITRAN values by 3.6, 6.9 and 3.4 %, respectively. Finally, very recently, a CIA measurement was performed by CRDS near the S2 (1–0) line at 4917 cm$^{-1}$ and a close agreement (0.7 %) with HITRAN value was obtained [31]. In summary, in view of the available experimental data, the deviations have an opposite sign in the (1–0) and (2–0) bands, their amplitude being larger in the (2–0) band. A systematic study of the (1–0) CIA over a wide spectral range remains to be undertaken.

## 4. Concluding remarks

The binary absorption coefficients of the $H_2$ CIA have been derived by cavity ring down spectroscopy (CRDS) over a wide range of the (2–0) band (7974- 8650 cm$^{-1}$). The sensitivity of the CRDS technique allowed for accurate measurements at subatmospheric pressures while previous studies have used $H_2$ densities of several tens of amagat or more. The obtained binary coefficients are reported with a 1.5 % accuracy and supported by a careful checking of the quadratic pressure dependence of the CIA during pressure ramps up to 1 atm. The comparison to theory [7, 12] shows an underestimation of the calculated values ranging between 5 and 25 %, largely exceeding the experimental error bars. The impact of such differences in the opacity in dense planetary atmospheres and "cool" stellar objects remains to be estimated.

In the present work, the sampling measurements points were selected distant from the $H_2$ lines. The weak Q1–Q4, S0, and S1 electric-quadrupole transitions of $H_2$ (included in Fig. 5) were very recently measured at room temperature by comb-referenced cavity ring-down spectroscopy (CR-CRDS) [33]. Their accurate transition frequencies were determined by applying a multi-spectrum fit procedure with a sophisticated profile model including speed-dependent collisional broadening and shifting phenomena. The performances of the developed

CR-CRDS setup (noise equivalent absorption, $\alpha_{min}$, smaller than $10^{-11}$ $cm^{-1}$) allowed for the measurement of the Q1, S0, and S1 lines with an $H_2$ pressure of a few Torr. We plan to use this setup to investigate in more details the CIA around the $H_2$ quadrupole lines. Indeed, in the fundamental band, especially near the Q lines, intercollisional interference effect causes a sharp drop of the CIA absorption [34–37]. The phenomenon may be enhanced in mixtures of $H_2$ with foreign gases (He, $N_2$, Ar…) [5,34,38–40]. These "intercollisional dips" have been interpreted as resulting from the correlation of dipoles induced in subsequent collisions leading to destructive interference. At the considerable densities used in most of the measurements, the "intercollisional dips" are broad and obscure the absorption of the $H_2$ quadrupole lines. In a series of high resolution FTS spectra recorded at pressures limited to 2.7 atm, Kelley and Bragg observed the narrow (1–0) Q1, Q2 and S0 lines superimposed to relatively narrow intercollisional dips (FWHM ~0.2 $cm^{-1}$) [35]. Interestingly, none of the studies of the (2–0) CIA reviewed in Table 1 has evidenced a spectral signature of intercollisional interference dips. A tentative theoretical explanation of the weakness of intercollisional interferences in the (2–0) band has been proposed in [10]. Nevertheless, considering the sensitivity provided nowadays by the CRDS technique, we plan to reconsider this issue experimentally by recording series of high resolution spectra around the (2–0) lines, over spectral intervals of a few $cm^{-1}$, thus significantly extended compared to the recordings of Ref. [33].

## CRediT authorship contribution statement

**A.O. Koroleva:** Writing – original draft, Investigation, Formal analysis, Data curation. **S. Kassi:** Software, Methodology, Investigation, Data curation. **H. Fleurbaey:** Writing – review & editing, Investigation, Data curation. **A. Campargue:** Writing – original draft, Investigation.

## Declaration of competing interest

The authors declare that they have no known competing financial interests or personal relationships that could have appeared to influence the work reported in this paper.

## Data availability

Data will be made available on request.

## Acknowledgments

AOK acknowledges the support by the French National Research Agency in the framework of the "Investissements d'avenir" program (ANR-15-IDEX-02) and partial support from the Russian State Project No.FFUF-2024-0016. The support by CNRS (France) in the frame of the International Research Project SAMIA is acknowledged.

## References

[1] Welsh HL, Crawford MF, MacDonald JCF, Chisholm DA. Induced infrared absorptions of $H_2$, $N_2$, and $O_2$ in the first overtone regions. Phys Rev 1951;83(6):1264.
[2] Herzberg G. Spectroscopic evidence of molecular hydrogen in the atmospheres of Uranus and Neptune. Astrophys J 1952;115:337–40 (1952), 115, 337-340.
[3] Van Kranendonk J. Theory of induced infra-red absorption. Physica 1957;23(6–10):825–37.
[4] Van Kranendonk J. Induced infra-red absorption in gases: calculation of the binary absorption coefficients of symmetrical diatomic molecules. Physica 1958;24(1–5):347–62.
[5] Van Kranendonk J. Intercollisional interference effects in pressure-induced infrared spectra. Can J Phys 1968;46(10):1173–9.
[6] Poll JD, Hunt JL. On the moments of the pressure-induced spectra of gases. Can J Phys 1976;54(5):461–70.
[7] Abel M, Frommhold L, Li X, Hunt KL. Collision-induced absorption by $H_2$ pairs: from hundreds to thousands of Kelvin. J Phys Chem A 2011;115(25):6805–12.
[8] Abel M, Frommhold L. Collision-induced spectra and current astronomical research. Can J Phys 2013;91(11):857–69.
[9] Meyer W, Borysow A, Frommhold L. Absorption spectra of $H_2$-$H_2$ pairs in the fundamental band. Phys Rev A 1989;40(12):6931.
[10] Meyer W, Borysow A, Frommhold L. Collision-induced first overtone band of gaseous hydrogen from first principles. Phys Rev A 1993;47(5):4065.
[11] Borysow A, Borysow J, Fu Y. Semi-empirical model of collision-induced absorption spectra of $H_2$–$H_2$ complexes in the second overtone band of hydrogen at temperatures from 50 to 500K. Icarus 2000;145(2):601–8.
[12] Borysow A. Collision-induced absorption coefficients of $H_2$ pairs at temperatures from 60K to 1000K. Astron Astrophys 2002;390(2):779–82.
[13] Frommhold L. Collision-induced absorption in gases. Cambridge, NY: Cambridge University Press; 1993. and 2006.
[14] Karman T, van der Avoird A, Groenenboom GC. Collision-induced absorption with exchange effects and anisotropic interactions: theory and application to $H_2$− $H_2$. J Chem Phys 2015;(8):142.
[15] Brodbeck C, Bouanich JP, Van-Thanh N, Borysow A. The binary collision-induced first overtone band of gaseous hydrogen. In: Proceedings of the AIP conference. 559. American Institute of Physics; 2001. p. 433–5.
[16] Watanabe A, Hunt JL, Welsh HL. Structure of the pressure-induced infrared spectrum of hydrogen in the first overtone region. Can J Phys 1971;49(7):860–3.
[17] McKellar ARW, Welsh HL. Collision-induced spectra of hydrogen in the first and second overtone regions with applications to planetary atmospheres. Proc R Soc Lond 1971;322(1551):421–34. A. Mathematical and Physical Sciences.
[18] Silvaggio PM, Goorvitch D, Boese RW. Investigation of the 2-0 pressure-induced vibrational absorption spectrum of hydrogen at temperatures below ambient. J Quant Spectrosc Radiat Transf 1981;26(2):103–6.
[19] McKellar ARW. The collision-induced first-overtone band of hydrogen at low temperature. Can J Phys 1988;66(2):155–8.
[20] Kassi S, Campargue A. Electric quadrupole transitions and collision-induced absorption in the region of the first overtone band of $H_2$ near 1.25μm. J Mol Spectrosc 2014;300:55–9.
[21] Abu-Kharma M. Analysis of the collision-induced absorption spectra in the second overtone region of $H_2$–$H_2$ at 298K. J Mol Spectrosc 2015;308:48–50.
[22] Brodbeck C, Bouanich JP, Fu Y, Borysow A. Collision-induced absorption by $H_2$ pairs in the second overtone band at 298 and 77.5 K: comparison between experimental and theoretical results. J Chem Phys 1999;110(10):4750–6.
[23] Mondelain D, Boulet C, Hartmann JM. The binary absorption coefficients for $H_2$+ $CO_2$ mixtures in the 2.12–2.35μm spectral region determined by CRDS and by semi-empirical calculations. J Quant Spectrosc Radiat Transf 2021;260:107454.
[24] Gordon IE, Rothman LS, Hargreaves RJ, Hashemi R, Karlovets EV, Skinner, et al. The HITRAN2020 molecular spectroscopic database. J Quant Spectrosc Radiat Transf 2022;277:107949.
[25] Romanini D, Kachanov AA, Sadeghi N, Stoeckel F. CW cavity ring down spectroscopy. Chem Phys Lett 1997;264(3–4):316–22.
[26] Berden G, Peeters R, Meijer G. Cavity ring-down spectroscopy: experimental schemes and applications. Int Rev Phys Chem 2000;19(4):565–607.
[27] Kassi S, Campargue A. Cavity ring down spectroscopy with 5× 10− 13 cm− 1 sensitivity. J Chem Phys 2012;137(23).
[28] Koroleva AO, Kassi S, Campargue A. The water vapor self-continuum absorption at room temperature in the 1.25μm window. J Quant Spectrosc Radiat Trans 2022;286:108206.
[29] Dalgarno A, Williams DA. Rayleigh scattering by molecular hydrogen. Astrophys J 1962;136:690–2. vol. 136690-692.
[30] Campargue A, Kassi S, Pachucki K, Komasa J. The absorption spectrum of H 2: CRDS measurements of the (2-0) band, review of the literature data and accurate ab initio line list up to 35000 cm− 1. Phys Chem Chem Phys 2012;14(2):802–15.
[31] Mondelain D, de Casson LB, Fleurbaey H, Kassi S, Campargue A. Accurate absolute frequency measurement of the S (2) transition in the fundamental band of H 2 near 2.03μm. Phys Chem Chem Phys 2023;25(34):22662–8.
[32] Thalman R, Zarzana KJ, Tolbert MA, Volkamer R. Rayleigh scattering cross-section measurements of nitrogen, argon, oxygen and air. J Quant Spectrosc Radiat Trans 2014;147:171–7.
[33] Fleurbaey H, Koroleva AO, Kassi S, Campargue A. The high-accuracy spectroscopy of H 2 rovibrational transitions in the (2-0) band near 1.2μm. Phys Chem Chem Phys 2023;25(21):14749–56.
[34] Reddy SP. Phenomena induced by intermolecular interactions. New York: Plenum; 1985. edited by G. BirnbaumVolume 127, pp. 129–167 ISBN : 978-1-4612-9518-1.
[35] Kelley JD, Bragg SL. Effect of collisions on line profiles in the vibrational spectrum of molecular hydrogen. Phys Rev A 1986;34(4):3003.
[36] Bouanich JP, Brodbeck C, Drossart P. Collision-induced absorption by $H_2$-$H_2$ and $H_2$-He pairs in the fundamental band—an experimental study. J Quant Spectrosc Radiat Transf 2020;44(4):393–403.
[37] Welsh HL. The pressure-induced infrared spectrum of hydrogen and its application to the study of planetary atmospheres. J Atmos Sci 2020;26(5):835–40.
[38] McKellar ARW, Mactaggart JW, Welsh HL. Studies in molecular dynamics by collision induced infrared absorption in $H_2$–rare gas mixtures. III. $H_2$–He mixtures at low temperatures and densities. Can J Phys 1975;53(19):2060–7.
[39] Mactaggart JW, Welsh HL. Studies in molecular dynamics by collision-induced infrared absorption in $H_2$–rare gas mixtures. I. profile analysis and the intercollisional interference effect. Can J Phys 1973;51(2):158–69.
[40] Poll JD, Hunt JL, Mactaggart JW. Intercollisional interference in the S lines of $H_2$–He mixtures. Can J Phys 1975;53(10):954–61.